SLAC-PUB-8813
April 19, 2002

Precision Measurement of the Proton and Deuteron Spin Structure Functions g$_2$ and Asymmetries A$_2$*

The E155 Collaboration

P. L. Anthony,[12] R. G. Arnold,[1,††] T. Averett,[15] H. R. Band,[16] N. Benmouna,[1] W. Boeglin,[5] H. Borel,[4] P. E. Bosted,[1,††] S. L. Bültmann,[14,§§] G. R. Court,[6] D. Crabb,[14] D. Day,[14] P. Decowski,[11] P. DePietro,[1] H. Egiyan,[15] R. Erbacher,[12,∞] R. Erickson,[12] R. Fatemi,[14] E. Frlez,[14] K. A. Griffioen,[15] C. Harris,[14] E. W. Hughes,[2] C. Hyde-Wright,[9] G. Igo,[3] J. Johnson,[12] P. King,[15] K. Kramer,[15] S. E. Kuhn,[9] D. Lawrence,[8] Y. Liang,[1] R. Lindgren,[14] R. M. Lombard-Nelsen,[4] P. McKee,[14] D.E. McNulty,[14] W. Meyer,[14,♭] G. S. Mitchell,[16,§] J. Mitchell,[13] M. Olson,[10] S. Penttila,[7] G. A. Peterson,[8] R. Pitthan,[12] D. Pocanic,[14] R. Prepost,[16] C. Prescott,[12] B. A. Raue,[5] D. Reyna,[1,♡] P. Ryan,[15] L. S. Rochester,[12] S. Rock,[1,††] O. Rondon-Aramayo,[14] F. Sabatie,[9,♠] T. Smith,[7] L. Sorrell,[1] S. St.Lorant,[12] Z. Szalata,[1,†] Y. Terrien,[4] A. Tobias,[14] T. Toole,[1,‡] S. Trentalange,[3] F. R. Wesselmann,[9] T. R. Wright,[16] M. Zeier,[14] H. Zhu,[14] B. Zihlmann[14]

[1] *American University, Washington, D.C. 20016*
[2] *California Institute of Technology, Pasadena, California 91125*
[3] *University of California, Los Angeles, California 90095*
[4] *DAPNIA-Service de Physique Nucleaire, CEA-Saclay, F-91191 Gif/Yvette Cedex, France*
[5] *Florida International University, Miami, Florida 33199.*
[6] *University of Liverpool, Liverpool L69 3BX, United Kingdom*
[7] *Los Alamos National Laboratory, Los Alamos, New Mexico 87545*
[8] *University of Massachusetts, Amherst, Massachusetts 01003*
[9] *Old Dominion University, Norfolk, Virginia 23529*
[10] *St. Norbert College, De Pere, WI 54115*
[11] *Smith College, Northampton, Massachusetts 01063*
[12] *Stanford Linear Accelerator Center, Stanford, California 94309*
[13] *Thomas Jefferson National Accelerator Facility, Newport News, Virginia 23606*
[14] *University of Virginia, Charlottesville, Virginia 22901*
[15] *The College of William and Mary, Williamsburg, Virginia 23187*
[16] *University of Wisconsin, Madison, Wisconsin 53706*

To be submitted to Physical Review Letters

We have measured the spin structure functions g_2^p and g_2^d and the virtual photon asymmetries A_2^p and A_2^d over the kinematic range $0.02 \leq x \leq 0.8$ and $0.7 \leq Q^2 \leq 20$ GeV^2 by scattering 29.1 and 32.3 GeV longitudinally polarized electrons from transversely polarized NH_3 and ^{6}LiD targets. Our measured g_2 approximately follows the twist-2 Wandzura-Wilczek calculation. The twist-3 reduced matrix elements d_2^p and d_2^n are less than two standard deviations from zero. The data are inconsistent with the Burkhardt-Cottingham sum rule if there is no pathological behavior as $x \to 0$. The Efremov-Leader-Teryaev integral is consistent with zero within our measured kinematic range. The absolute value of A$_2$ is significantly smaller than the $A_2 < \sqrt{R(1+A_1)/2}$ limit.

The deep inelastic spin structure functions of the nucleons, $g_1(x, Q^2)$ and $g_2(x, Q^2)$, depend on the spin distribution of the partons and their correlations. The function g_1 can be primarily understood in terms of the quark parton model (QPM) and perturbative QCD with higher twist terms at low Q^2. The function g_2 is of particular interest since it has contributions from quark-gluon correlations and other higher twist terms at leading order in Q^2 which cannot be

*Work supported by Department of Energy contract DE–AC03–76SF00515.

described perturbatively. By interpreting g_2 using the operator product expansion (OPE) [1,2], it is possible to study contributions to the nucleon spin structure beyond the simple QPM.

The structure function g_2 can be written [3]:

$$g_2(x,Q^2) = g_2^{WW}(x,Q^2) + \overline{g_2}(x,Q^2) \tag{1}$$

in which

$$g_2^{WW}(x,Q^2) = -g_1(x,Q^2) + \int_x^1 \frac{g_1(y,Q^2)}{y}dy,$$
$$\overline{g_2}(x,Q^2) = -\int_x^1 \frac{\partial}{\partial y}\left(\frac{m}{M}h_T(y,Q^2) + \xi(y,Q^2)\right)\frac{dy}{y},$$

x is the Bjorken scaling variable and Q^2 is the absolute value of the virtual photon four-momentum squared. The twist-2 term g_2^{WW} was derived by Wandzura and Wilczek [4] and depends only on g_1 [5–10]. The function $h_T(x,Q^2)$ is an additional twist-2 contribution [3,11] that depends on the transverse polarization density in the nucleon. The h_T contribution to $\overline{g_2}$ is suppressed by the ratio of the quark to nucleon masses m/M [11] and its effect is thus small for up and down quarks and is assumed negligible in the theoretical models referenced in this paper. The twist-3 part (ξ) comes from quark-gluon correlations and is the main focus of our study.

Low-precision measurements of g_2 and A_2 exist for the proton and deuteron [12–14], as well as for the neutron [7,15]. In this Letter, we report new, precise measurements of g_2 and A_2 for the proton and deuteron.

Electron beams with energies of 29.1 and 32.3 GeV and longitudinal polarizations of $P_b = (83.2 \pm 3.0)\%$ struck approximately transversely polarized NH_3 [6] (average polarization $< P_t >= 0.70$) or ^{6}LiD [16] ($< P_t >= 0.22$) targets. The beam helicity was randomly chosen pulse by pulse. Scattered electrons were detected in three independent spectrometers centered at 2.75°, 5.5°, and 10.5°. The two small-angle spectrometers were the same as in SLAC E155 [9], while the large-angle spectrometer had additional hodoscopes and a more efficient pre-radiator shower counter. Further information on the experimental apparatus can be found in references [6,8,9]. The approximately equal amounts of data taken with the two beam energies and opposites signs of target polarization gave consistent results.

The measured asymmetry, $\tilde{A_\perp}$, differs from $A_\perp$ because the target polarizations were not exactly perpendicular to the beam line. For each kinematic bin $\tilde{A_\perp}$ was formed using

$$\tilde{A_\perp} = \frac{1}{f_{RC}}\left[\frac{C_1}{fP_t}\left(\left(\frac{N_L - N_R}{N_L + N_R}\right)\frac{1}{P_b} - A_{EW}\right) + C_2\right] + A_{RC} \tag{2}$$

where N_L and N_R are the measured counting rates from the two beam helicities, including small corrections for pion and charge symmetric backgrounds, dead-time and tracking efficiency, and A_{EW} is the electroweak asymmetry ($\approx 8 \times 10^{-5}Q^2$). The target dilution factor, f, is the fraction of free polarizable protons (≈ 0.13) or deuterons (≈ 0.18) for a given spectrometer acceptance. For the proton target, the nuclear correction $C_1 \approx 0.98$ is due to the polarization of the ^{15}N and C_2=0. The deuteron data were extracted from the ^{6}LiD results by applying a slightly x-dependent nuclear correction $C_1 \approx 0.52$ to account for the lithium and deuterium nuclear wave functions with ^{6}Li$\sim$ $\alpha + d$ [16]. An additional correction $C_2(x)\sigma_p/\sigma_d\tilde{A_\perp^p}$, ($C_2 \approx -0.042$) accounts for the $\sim$ 4% polarized ^{7}Li in the target. The quantities f_{RC} and A_{RC} are radiative corrections determined using a method similar to E143 [6]. The quantity $1 - f_{RC}$ was calculated as the proportion of events in a bin coming from elastic and quasi-elastic tails, and A_{RC} included polarization-dependent elastic and quasi-elastic as well as inelastic and vertex corrections. The radiative dilution factor f_{RC} has the effect of increasing the statistical errors at low x. Uncertainties in the radiative corrections were estimated by varying the input models over a range consistent with the measured data.

The detailed results for $\tilde{A_\perp}$ are shown in Table I. Because $\tilde{A_\perp}$ is close to zero, the relative statistical errors are always greater than 25%. The uncertainties due to target and beam polarization and dilution factor combined are 5.1% (proton) and 6.2% (deuteron). They are multiplicative and small compared to the statistical errors. The total systematic error is also shown in Table I.

We determined $g_2(x,Q^2)$ and $A_2(x,Q^2)$ from $\tilde{A_\perp}$ (dominant contribution) and the previously measured g_1 (small contribution) using:

$$g_2 = \frac{yF_1}{2E'(\cos\Theta - \cos\alpha)}\left[\tilde{A_\perp}\nu\frac{(1+\epsilon R)}{1-\epsilon} - \frac{g_1}{F_1}[E\cos\alpha + E'\cos\Theta]\right] \tag{3}$$
$$A_2 = \gamma(g_1 + g_2)/F_1 \tag{4}$$

where $\cos\Theta = \sin\alpha\sin\theta\cos\Phi + \cos\alpha\cos\theta$, θ is the spectrometer angle, Φ is the angle between the spin plane and the scattering plane, $\alpha = 92.4°$ is the angle of the target polarization with respect to the beam direction, $y = \nu/E$, $\nu = E - E'$, E and E' are the incident and scattered electron energies, $\epsilon^{-1} = 1 + 2\left[1 + 1/\gamma^2\right]\tan^2(\theta/2)$, $\gamma = \sqrt{Q^2/\nu^2}$ and $F_1 = F_2(1 + 4M^2x^2/Q^2)/[2x(1 + R)]$. We used a new Q^2-dependent parameterization of g_1 [9] world data, the NMC fit to $F_2(x, Q^2)$ [17] and the SLAC fit to $R(x, Q^2) = \sigma_L/\sigma_T$ [18]. The structure functions for p, d, and n are related by $g_2^d = (g_2^p + g_2^n)(1 - 1.5\omega_D)/2$, where $\omega_D = 0.05$, the fraction of D-wave in the deuteron wave function.

Results for A_2 and xg_2 for the three spectrometers and two energies are given in Table II with statistical errors. The systematic error on xg_2 is much smaller than the statistical error and is given approximately by $a + bx$ where $a_p(a_d)$=0.0016 (0.0009) and $b_p(b_d)$=−0.0012 (−0.0008). It includes the systematic errors on $\tilde{A}_\perp$ as well as a 5% normalization uncertainty on g_1. The data cover the kinematic range $0.02 \le x \le 0.8$ and $0.7 \le Q^2 \le 20$ GeV^2 with an average Q^2 of 5 GeV^2. Figure 1 shows the values of xg_2 as a function of Q^2 for several values of x along with results from E143 [6] and E155 [14]. The data approximately follow the Q^2 dependence of g_2^{WW} (solid curve), although for the proton, the data points are lower than g_2^{WW} at low and intermediate x and higher at high x. The predictions of Stratmann [19] are closer to the data.

To get average values at the average Q^2 for each x bin we used the Q^2 dependence of g_2^{WW}: $g_2(Q^2_{avg}) = g_2(Q^2_{exp}) - g_2^{WW}(Q^2_{exp}) + g_2^{WW}(Q^2_{avg})$. These averaged results for A_2 and xg_2 are listed at the bottom of Table II. Figure 2 shows the averaged xg_2 of this experiment along with xg_2^{WW} calculated using our parameterization of g_1. The combined new data for p disagree with g_2^{WW} with a χ^2/dof of 3.1 for 10 degrees of freedom. For d the new data agree with g_2^{WW} with a χ^2/dof of 1.2 for 10 dof. The data for g_2^p are also inconsistent with zero (χ^2/dof=15.5) while g_2^d differs from zero only at $x \sim 0.4$. Also shown in Fig. 2 is the Bag Model calculation of Stratmann [19] which is in good agreement with the data, a chiral soliton model calculation [20] which is too negative at $x \sim 0.4$ and the Bag Model calculation of Song [11] which is in clear disagreement with the data.

The average values of $A_2(x)$, shown in Fig. 3, are consistent with zero at low x, increasing to about 0.1 at the highest x, significantly different than zero. A_2^p is many standard deviations lower than the Soffer limit [22] of $|A_2| < \sqrt{R(1 + A_1)/2} \approx 0.4$ for all values of x. The same is true for A_2^d, except at the highest x value where the error is large.

The OPE allows us to write the hadronic matrix element in deep inelastic scattering in terms of a series of renormalized operators of increasing twist [1,2]. The moments of g_1 and g_2 for even $n \ge 2$ at fixed Q^2 can be related to twist-3 reduced matrix element, d_n, and higher twist terms which are suppressed by powers of $1/Q$. Neglecting quark mass terms we find that:

$$d_n = 2\int_0^1 dx\ x^n\left[\frac{n+1}{n}g_2(x, Q^2) + g_1(x, Q^2)\right] = 2\frac{n+1}{n}\int_0^1 dx\ x^n\overline{g_2}(x, Q^2). \qquad (5)$$

This relation is true to all orders of α_s [23]. The matrix element d_n measures deviations of g_2 from the twist-2 g_2^{WW} term. Note that some authors [2,24] define d_n with an additional factor of two. We calculated d_n using $d_2 = 3\int_0^1 dx\ x^2\overline{g_2}(x, Q^2)$ (see eq.5) with the assumption that $\overline{g_2}$ is independent of Q^2 in the measured region. This is not unreasonable since d_n depends only logarithmically on Q^2 [1]. The part of the integral for x below the measured region was assumed to be zero because of the x^2 suppression. For $x \ge 0.8$ we used $\overline{g_2} \propto (1 - x)^m$ where m=2 or 3, normalized to the data for $x \ge 0.5$. Because $\overline{g_2}$ is small at high x, the contribution was negligible for both cases. We obtained values of d_2^p =0.0025 ±0.0016 ±0.0010 and d_2^d =0.0054 ±0.0023 ±0.0005 at an average Q^2 of 5 GeV^2. We combined these results with those from SLAC experiments on the neutron (E142 [7] and E154 [15]) and proton and deuteron (E143 [6] and E155 [14]) to obtained average values d_2^p =0.0032 ±0.0017 and d_2^n =0.0079 ±0.0048 . These are consistent with zero (no twist-3) to within 2 standard deviations. The values of the 2^{nd} moments alone are: $\int_0^1 dx\ x^2 g_2(x, Q^2)$=−0.0072 ± 0.0005 ±0.0003 (p) and −0.0019 ± 0.0007 ±0.0001 (d).

Figure 4 shows the experimental values of d_2 for proton and neutron with their error, plotted along with theoretical models from left to right: Bag Models (Song [11], Stratmann [19], and Ji [25]); sum rules (Stein [26], BBK [27], Ehrnsperger [28]); chiral soliton models [20,21]; and lattice QCD calculations ($Q^2 = 5$ GeV^2, $\beta = 6.4$) [24]. The lattice and chiral calculations are in good agreement with the proton data and two standard deviations below the neutron data. The sum rule calculations are significantly lower than the data. The Non Singlet $3 \cdot (d_2^p - d_2^n) =$ −0.0141 ±0.0170 is consistent with an instanton vacuum calculation of ~ 0.001 [29].

The Burkhardt-Cottingham sum rule [30] for g_2 at large Q^2, $\int_0^1 g_2(x)dx = 0$, was derived from virtual Compton scattering dispersion relations. It does not follow from the OPE since $n = 0$. Its validity depends on the lack of singularities for g_2 at $x = 0$, and a dramatic rise of g_2 at low x could invalidate the sum rule [31]. We evaluated the Burkhardt-Cottingham integral in the measured region of $0.02 \le x \le 0.8$ at $Q^2 = 5$ GeV^2. The results for the proton and deuteron are −0.044 ±0.008 ±0.003 and −0.008 ±0.012 ±0.002 respectively. Averaging with the E143 and E155 results which cover a slightly more restrictive x range gives -0.042 ± 0.008 and -0.006 ± 0.011. This does not represent a conclusive test of the sum rule because the behavior of g_2 as $x \to 0$ is not known. However, if we assume that $g_2 = g_2^{WW}$ for $x < 0.02$, and use the relation $\int_0^x g_2^{WW}(y)dy = x\left[g_2^{WW}(x) + g_1(x)\right]$, there is an additional contribution of 0.020 (0.004) for the proton (deuteron).

The Efremov-Leader-Teryaev (ELT) sum rule [32] involves the valence quark contributions to g_1 and g_2: $\int_0^1 x[g_1^V(x) + 2g_2^V(x)]dx = 0$. Assuming that the sea quarks are the same in protons and neutrons, the sum rule takes a form $\int_0^1 x[g_1^p(x) + 2g_2^p(x) - g_1^n(x) - 2g_2^n(x)]dx = 0$. We evaluated this ELT integral in the measured region using our g_2 data and the fit to g_1. The result at $Q^2 = 5$ GeV^2 is $-0.013 \pm 0.008 \pm 0.002$, which is consistent with the expected value of zero. Including the data of E143 [6] and E155 [14] leads to -0.011 ± 0.008. The extrapolation to x=0 is not known, but is suppressed by a factor of x.

In summary, our results for g_2 follow approximately the twist-2 g_2^{WW} shape, but deviate significantly at some values of x. The values obtained for the twist-3 matrix element d_2 from this measurement and the SLAC average are less than two standard deviations from zero. The data over the measured range are inconsistent with the Burkhardt-Cottingham sum rule if there is no pathological behavior as $x \to 0$. The ELT integral is consistent with zero within our measured kinematic range.

We wish to thank the personnel of the SLAC accelerator and Experimental Facilities Departments for their efforts which resulted in the successful completion of the E155X experiment. This work was supported by the Department of Energy; the National Science Foundation; and the Centre National de la Recherche Scientifique and the Commissariat a l'Energie Atomique (French groups).

---

†† Present Address: University of Massachusetts, Amherst, MA 01003
§§ Present Address: Brookhaven National Laboratory, Upton, NY 11973
∞ Present Address: Fermi National Accelerator Laboratory, Batavia, IL 60510
♭ Present Address: Ruhr-Universität Bochum, Bochum, Germany
§ Present Address: Los Alamos National Laboratory, Los Alamos, NM 87545
♡ Present Address: Argonne National Laboratory, Argonne, IL 60439
♠ Present Address:DAPNIA-Service de Physique Nucleaire, CEA-Saclay, F-91191 Gif/Yvette Cedex, France
† Present Address: Stanford Linear Accelerator Center, Stanford, CA 94305
‡ Present Address: U. of Maryland, College Park, MD 20742
[1] E. Shuryak and A. Vainshtein, Nuc. Phys. B **201**, 141 (1982).
[2] R. Jaffe and X. Ji, Phys. Rev. D **43**, 724 (1991).
[3] J. L. Cortes, B. Pire and J. P. Ralston, Z. Phys. C **55**, 409 (1992).
[4] S. Wandzura and F. Wilczek, Phys. Lett. B **72**, 195 (1977).
[5] SMC: B. Adeva *et al.*, Phys. Rev. D **58**, 112001 (1998).
[6] E143: K. Abe *et al.*, Phys. Rev. D **58**, 112003 (1998).
[7] E142: P. Anthony *et al.* Phys. Rev. D **54**, 6620 (1996).
[8] E154: K. Abe *et al.*, Phys. Rev. Lett. **79**, 26 (1997).
[9] E155: P. Anthony *et al.*, Phys. Lett. B **463**, 339 (1999); B **493**, 19 (2000).
[10] HERMES: K. Ackerstaff *et al.* Phys. Lett. B **404**, 383 (1997); A. Airapetian *et al.*, Phys. Lett. B **442**, 484 (1998).
[11] X. Song, Phys. Rev. D **54**, 1955 (1996).
[12] SMC: D. Adams *et al.*, Phys. Lett. B **336**, 125 (1994); **396**, 338 (1997).
[13] E143: K. Abe *et al.*, Phys. Rev. Lett. **76**, 587 (1996).
[14] E155: P. Anthony *et al.*, Phys. Lett. B **458**, 529 (1999).
[15] E154: K. Abe *et al.*, Phys. Lett. B **404**, 377 (1997).
[16] S. Bültmann *et al.*, Nucl. Inst. Meth. A **425**, 23 (1999).
[17] NMC: M. Arneodo *et al.*, Phys. Lett. B **364**, 107 (1995).
[18] E143: K. Abe *et al.*, Phys. Lett. B **452**, 194 (1999).
[19] M. Stratmann, Z. Phys. C **60**, 763 (1993).
[20] H. Weigel and L. Gamberg, Nucl. Phys. A **680**, 48 (2000).
[21] M. Wakamatsu, Phys. Lett. B **487**, 118 (2000).
[22] J. Soffer and O. V. Teryaev, Phys. Lett. B **490**, 106 (2000).
[23] X. Ji and J. Osborne, Nucl. Phys. B **608**, 235 (2001).

[24] M. Göckeler *et al.*, Phys. Rev. D **63**, 074506 (2001).
[25] X. Ji and P. Unrau, Phys. Lett. B **333**, 228 (1994).
[26] E. Stein *et al.*, Phys. Lett. B **343**, 369 (1995).
[27] I. Balitsky, V. Braun and A. Kolesnichenko, Phys. Lett. B **242**, 245 (1990); **318**, 648 (1993) (Erratum).
[28] B. Ehrnsperger and A. Schafer, Phys. Rev. D **52**, 2709 (1995).
[29] J. Balla, M.V. Polyakov, and C. Weiss, Nucl. Phys. B **510**, 327 (1998).
[30] H. Burkhardt and W. N. Cottingham, Ann. Phys. **56**, 453 (1970).
[31] I. P. Ivanov *et al.*, Phys. Rep. **320**, 175 (1999).
[32] A. V. Efremov, O. V. Teryaev and E. Leader, Phys. Rev. D**55**, 4307 (1997).

TABLE I. Results for $\tilde{A_\perp}$ with statistical and systematic errors for proton and deuteron at the measured x and Q^2 [GeV^2]. Also shown are the additive and multiplicative radiative corrections

x	$< Q^2 >$	$\tilde{A_\perp}^{\,p}$	f^p_{RC}	A^p_{RC}	$\tilde{A_\perp}^{\,d}$	f^d_{RC}	A^d_{RC}
		$\theta \approx 2.75°$; E=29.1 GeV					
0.017	0.63	8.611 ± 4.785±0.456	0.811	-0.001	5.545 ± 4.476±NaN	0.877	0.000
0.020	0.71	0.025 ± 0.015±0.001	0.841	-0.001	0.018 ± 0.022±0.001	0.896	0.000
0.022	0.76	0.004 ± 0.007±0.000	0.861	-0.001	−0.006 ± 0.010±0.001	0.909	0.000
0.024	0.82	0.000 ± 0.005±0.000	0.880	-0.001	−0.003 ± 0.008±0.000	0.922	0.000
0.027	0.86	0.008 ± 0.005±0.000	0.904	-0.001	−0.007 ± 0.008±0.001	0.937	0.000
0.031	0.91	0.001 ± 0.005±0.000	0.921	-0.001	0.006 ± 0.008±0.000	0.948	0.000
0.035	0.96	−0.002 ± 0.005±0.000	0.935	-0.001	0.008 ± 0.008±0.001	0.957	0.000
0.039	1.02	−0.011 ± 0.005±0.001	0.946	-0.001	0.000 ± 0.008±0.000	0.957	0.000
0.044	1.07	−0.015 ± 0.005±0.001	0.954	-0.001	0.008 ± 0.007±0.001	0.970	0.000
0.049	1.13	−0.008 ± 0.005±0.000	0.962	-0.001	−0.003 ± 0.007±0.000	0.975	-0.001
0.056	1.18	−0.004 ± 0.005±0.000	0.967	-0.001	0.009 ± 0.007±0.001	0.978	-0.001
0.063	1.23	−0.005 ± 0.005±0.000	0.971	-0.002	0.008 ± 0.007±0.001	0.981	-0.001
0.071	1.29	−0.010 ± 0.005±0.001	0.975	-0.002	0.010 ± 0.007±0.001	0.984	-0.001
0.079	1.34	−0.002 ± 0.005±0.000	0.979	-0.002	−0.004 ± 0.007±0.000	0.986	-0.001
0.089	1.40	−0.004 ± 0.005±0.000	0.981	-0.002	−0.006 ± 0.007±0.000	0.987	-0.001
0.101	1.45	0.006 ± 0.005±0.001	0.982	-0.002	0.007 ± 0.007±0.001	0.989	-0.001
0.113	1.50	0.002 ± 0.005±0.001	0.986	-0.002	−0.019 ± 0.007±0.001	0.990	-0.001
0.128	1.54	−0.005 ± 0.005±0.001	0.985	-0.002	0.002 ± 0.008±0.000	0.991	-0.001
0.144	1.59	−0.007 ± 0.005±0.001	0.986	-0.002	0.004 ± 0.008±0.000	0.991	-0.001
0.162	1.63	−0.003 ± 0.005±0.000	0.987	-0.002	0.002 ± 0.008±0.000	0.991	-0.001
0.182	1.67	−0.002 ± 0.005±0.000	0.987	-0.002	−0.007 ± 0.008±0.000	0.991	-0.001
0.205	1.71	0.009 ± 0.005±0.001	0.988	-0.002	0.000 ± 0.009±0.000	0.991	-0.001
0.230	1.74	−0.008 ± 0.006±0.001	0.987	-0.002	−0.003 ± 0.009±0.000	0.991	-0.001
0.259	1.77	0.001 ± 0.006±0.000	0.987	-0.002	−0.009 ± 0.009±0.001	0.991	-0.001
0.292	1.80	−0.011 ± 0.006±0.001	0.986	-0.002	0.003 ± 0.010±0.000	0.990	-0.001
0.329	1.83	−0.009 ± 0.006±0.001	0.983	-0.002	0.009 ± 0.010±0.001	0.989	-0.001
		$\theta \approx 5.5°$; E=29.1 GeV					
0.065	2.32	−0.013 ± 0.053±0.001	0.951	0.002	−0.023 ± 0.076±0.001	0.965	0.001
0.071	2.49	0.018 ± 0.022±0.001	0.958	0.003	0.042 ± 0.032±0.003	0.970	0.001
0.080	2.71	0.010 ± 0.014±0.001	0.967	0.003	0.049 ± 0.021±0.003	0.977	0.001
0.090	2.94	−0.011 ± 0.011±0.001	0.975	0.003	−0.008 ± 0.016±0.001	0.982	0.002
0.101	3.17	−0.004 ± 0.009±0.000	0.981	0.003	−0.010 ± 0.014±0.001	0.986	0.002
0.114	3.40	0.021 ± 0.008±0.001	0.986	0.003	−0.013 ± 0.013±0.001	0.989	0.002
0.128	3.62	0.011 ± 0.008±0.001	0.989	0.003	0.000 ± 0.012±0.000	0.992	0.002
0.144	3.85	−0.017 ± 0.008±0.001	0.991	0.003	0.004 ± 0.012±0.000	0.994	0.002
0.162	4.08	−0.016 ± 0.007±0.001	0.994	0.003	0.000 ± 0.011±0.000	0.995	0.002
0.182	4.31	−0.009 ± 0.007±0.001	0.995	0.003	0.017 ± 0.012±0.001	0.996	0.002
0.205	4.53	−0.010 ± 0.008±0.001	0.996	0.003	0.021 ± 0.012±0.001	0.997	0.002
0.231	4.74	−0.020 ± 0.008±0.001	0.997	0.003	−0.002 ± 0.013±0.000	0.998	0.002
0.259	4.94	0.004 ± 0.009±0.001	0.998	0.003	0.001 ± 0.014±0.001	0.998	0.002
0.292	5.14	−0.018 ± 0.009±0.001	0.998	0.003	−0.027 ± 0.015±0.002	0.999	0.001
0.328	5.32	−0.018 ± 0.010±0.001	0.998	0.002	0.008 ± 0.016±0.001	0.999	0.001
0.370	5.50	−0.048 ± 0.011±0.002	0.998	0.002	0.011 ± 0.018±0.001	0.999	0.001
0.416	5.66	−0.025 ± 0.012±0.001	0.999	0.002	−0.034 ± 0.020±0.002	0.999	0.001
0.468	5.82	−0.049 ± 0.013±0.003	0.998	0.002	0.020 ± 0.023±0.001	0.999	0.002
0.527	5.96	−0.034 ± 0.015±0.002	0.998	0.003	0.003 ± 0.027±0.000	0.998	0.002
0.592	6.09	−0.027 ± 0.018±0.001	0.997	0.003	−0.012 ± 0.033±0.001	0.998	0.003
0.667	6.20	−0.050 ± 0.022±0.003	0.995	0.001	−0.029 ± 0.041±0.002	0.996	0.001
0.750	6.31	−0.089 ± 0.029±0.005	0.990	0.001	0.025 ± 0.054±0.002	0.992	0.002
0.844	6.40	−0.088 ± 0.047±0.004	0.961	0.004	0.057 ± 0.076±0.004	0.972	0.004
		$\theta \approx 10.5°$; E=29.1 GeV					
0.129	5.36	−0.052 ± 0.031±0.003	0.963	-0.005	−0.028 ± 0.053±0.002	0.972	-0.002
0.144	5.89	−0.071 ± 0.025±0.004	0.970	-0.005	0.040 ± 0.045±0.003	0.977	-0.002
0.162	6.49	0.006 ± 0.022±0.001	0.977	-0.005	−0.015 ± 0.039±0.001	0.983	-0.002
0.182	7.17	0.012 ± 0.020±0.001	0.981	-0.005	0.045 ± 0.036±0.003	0.986	-0.003
0.205	7.91	−0.021 ± 0.020±0.001	0.986	-0.005	0.007 ± 0.036±0.001	0.989	-0.003
0.231	8.67	0.020 ± 0.021±0.001	0.989	-0.005	0.005 ± 0.039±0.001	0.992	-0.002
0.259	9.39	−0.025 ± 0.022±0.002	0.992	-0.005	−0.044 ± 0.043±0.003	0.993	-0.002
0.292	10.18	0.029 ± 0.024±0.002	0.993	-0.004	−0.040 ± 0.047±0.003	0.995	-0.002
0.328	10.96	−0.028 ± 0.026±0.002	0.995	-0.004	0.069 ± 0.053±0.004	0.996	-0.002
0.369	11.78	−0.014 ± 0.029±0.002	0.997	-0.004	−0.088 ± 0.061±0.006	0.997	-0.002
0.415	12.57	0.004 ± 0.034±0.002	0.997	-0.003	−0.027 ± 0.072±0.003	0.997	-0.002
0.467	13.36	0.067 ± 0.041±0.004	0.998	-0.003	−0.014 ± 0.088±0.003	0.998	-0.002
0.526	14.19	0.032 ± 0.051±0.002	0.998	-0.002	−0.026 ± 0.114±0.002	0.999	-0.002
0.592	15.02	0.052 ± 0.067±0.003	0.999	-0.002	0.137 ± 0.158±0.008	0.999	-0.002
0.666	15.77	−0.195 ± 0.094±0.010	0.999	-0.002	−0.045 ± 0.229±0.003	0.999	-0.002
0.749	16.48	0.114 ± 0.142±0.006	0.999	-0.002	−0.035 ± 0.347±0.002	0.999	-0.002
0.845	17.10	0.299 ± 0.259±0.015	0.997	-0.002	−1.237 ± 0.588±0.077	0.998	-0.003
		$\theta \approx 2.75°$; E=32.3 GeV					
0.018	0.75	0.071 ± 0.081±0.004	0.820	-0.001	−0.047 ± 0.110±0.003	0.882	0.000
0.020	0.81	−0.002 ± 0.009±0.000	0.835	-0.001	−0.010 ± 0.014±0.001	0.892	0.000

0.022	0.87	0.000 ± 0.005±0.000	0.861	-0.001	0.002 ± 0.008±0.000	0.908	0.000
0.024	0.93	−0.006 ± 0.005±0.000	0.883	-0.001	0.009 ± 0.008±0.001	0.925	0.000
0.027	0.99	0.003 ± 0.004±0.000	0.909	-0.001	−0.003 ± 0.008±0.000	0.939	0.000
0.031	1.05	0.000 ± 0.004±0.000	0.925	-0.001	0.007 ± 0.008±0.000	0.950	0.000
0.035	1.12	−0.004 ± 0.004±0.000	0.938	-0.001	−0.001 ± 0.008±0.000	0.959	0.000
0.039	1.19	−0.001 ± 0.004±0.000	0.938	-0.001	−0.001 ± 0.007±0.000	0.967	0.000
0.044	1.25	−0.004 ± 0.004±0.000	0.959	-0.001	−0.011 ± 0.007±0.001	0.973	0.000
0.049	1.32	0.000 ± 0.004±0.000	0.966	-0.001	−0.008 ± 0.007±0.000	0.977	0.000
0.056	1.39	−0.003 ± 0.004±0.000	0.968	-0.002	0.000 ± 0.007±0.000	0.981	-0.001
0.063	1.46	−0.008 ± 0.004±0.000	0.977	-0.002	−0.002 ± 0.007±0.000	0.983	-0.001
0.071	1.54	−0.006 ± 0.004±0.000	0.980	-0.002	−0.009 ± 0.007±0.001	0.987	-0.001
0.079	1.61	0.004 ± 0.004±0.000	0.982	-0.002	−0.002 ± 0.007±0.000	0.988	-0.001
0.089	1.68	−0.003 ± 0.004±0.000	0.985	-0.002	0.011 ± 0.007±0.001	0.990	-0.001
0.101	1.74	−0.005 ± 0.004±0.000	0.988	-0.002	0.001 ± 0.007±0.000	0.991	-0.001
0.113	1.81	−0.003 ± 0.005±0.000	0.988	-0.002	0.000 ± 0.007±0.000	0.992	-0.001
0.128	1.87	−0.003 ± 0.005±0.000	0.989	-0.002	−0.003 ± 0.008±0.000	0.993	-0.001
0.144	1.93	−0.002 ± 0.005±0.000	0.991	-0.002	−0.014 ± 0.008±0.001	0.994	-0.001
0.162	1.98	−0.007 ± 0.005±0.001	0.992	-0.002	−0.001 ± 0.008±0.000	0.994	-0.001
0.182	2.03	0.010 ± 0.005±0.001	0.993	-0.002	−0.004 ± 0.008±0.000	0.994	-0.001
0.205	2.08	−0.003 ± 0.005±0.000	0.992	-0.002	−0.008 ± 0.009±0.001	0.994	-0.001
0.230	2.13	0.004 ± 0.005±0.000	0.992	-0.002	−0.001 ± 0.009±0.000	0.994	-0.001
0.259	2.17	0.007 ± 0.005±0.000	0.992	-0.002	−0.008 ± 0.009±0.001	0.994	-0.001
0.292	2.21	0.002 ± 0.006±0.000	0.992	-0.002	0.009 ± 0.010±0.001	0.994	-0.001
0.329	2.26	−0.004 ± 0.006±0.000	0.990	-0.002	0.001 ± 0.010±0.000	0.993	-0.001
$\theta \approx 5.5°$; E=32.3 GeV							
0.059	2.48	−0.685 ± 0.248±0.035	0.940	0.002	0.205 ± 0.369±0.013	0.957	0.001
0.064	2.65	0.008 ± 0.029±0.001	0.949	0.002	0.022 ± 0.043±0.001	0.963	0.001
0.071	2.87	−0.019 ± 0.015±0.001	0.959	0.003	0.026 ± 0.023±0.002	0.969	0.001
0.080	3.13	0.004 ± 0.011±0.001	0.968	0.003	0.016 ± 0.017±0.001	0.976	0.001
0.090	3.41	0.004 ± 0.009±0.000	0.974	0.003	−0.005 ± 0.013±0.000	0.981	0.002
0.101	3.67	−0.012 ± 0.008±0.001	0.981	0.003	−0.005 ± 0.012±0.000	0.986	0.002
0.113	3.95	0.000 ± 0.007±0.001	0.985	0.003	−0.004 ± 0.011±0.000	0.989	0.002
0.128	4.22	−0.002 ± 0.007±0.001	0.991	0.003	0.011 ± 0.010±0.001	0.992	0.002
0.144	4.51	−0.005 ± 0.007±0.001	0.992	0.003	0.014 ± 0.010±0.001	0.994	0.002
0.162	4.79	0.002 ± 0.007±0.001	0.994	0.003	0.000 ± 0.010±0.000	0.995	0.002
0.182	5.07	−0.005 ± 0.007±0.001	0.995	0.003	0.002 ± 0.011±0.000	0.997	0.002
0.205	5.34	−0.003 ± 0.007±0.001	0.997	0.003	−0.001 ± 0.011±0.000	0.997	0.002
0.230	5.60	−0.023 ± 0.007±0.001	0.997	0.003	−0.006 ± 0.012±0.001	0.998	0.002
0.259	5.86	−0.007 ± 0.008±0.001	0.998	0.003	−0.001 ± 0.013±0.001	0.998	0.001
0.292	6.11	−0.022 ± 0.008±0.001	0.998	0.002	0.016 ± 0.014±0.001	0.999	0.001
0.328	6.34	−0.008 ± 0.009±0.001	0.999	0.002	−0.034 ± 0.015±0.002	0.999	0.001
0.370	6.57	−0.034 ± 0.010±0.002	0.999	0.002	−0.025 ± 0.017±0.002	0.999	0.001
0.416	6.79	−0.022 ± 0.011±0.001	0.999	0.002	−0.023 ± 0.019±0.002	0.999	0.001
0.468	6.99	−0.037 ± 0.012±0.002	0.999	0.002	−0.001 ± 0.022±0.001	0.999	0.001
0.527	7.19	−0.030 ± 0.014±0.002	0.999	0.002	−0.014 ± 0.026±0.001	0.999	0.002
0.592	7.36	−0.032 ± 0.016±0.002	0.998	0.003	−0.029 ± 0.032±0.002	0.999	0.002
0.667	7.53	−0.023 ± 0.020±0.001	0.997	0.005	−0.019 ± 0.041±0.001	0.998	0.004
0.750	7.66	−0.053 ± 0.026±0.003	0.994	0.002	0.040 ± 0.053±0.002	0.995	0.002
0.844	7.78	0.046 ± 0.042±0.002	0.980	0.003	−0.127 ± 0.074±0.008	0.983	0.003
$\theta \approx 10.5°$; E=32.3 GeV							
0.129	6.09	−0.014 ± 0.025±0.001	0.962	-0.005	0.010 ± 0.038±0.001	0.971	-0.002
0.144	6.71	0.014 ± 0.019±0.001	0.969	-0.006	−0.005 ± 0.031±0.001	0.977	-0.002
0.162	7.41	−0.036 ± 0.016±0.002	0.977	-0.005	−0.048 ± 0.027±0.003	0.982	-0.002
0.182	8.21	−0.017 ± 0.015±0.002	0.982	-0.005	−0.005 ± 0.024±0.001	0.986	-0.002
0.205	9.06	−0.024 ± 0.015±0.002	0.986	-0.005	0.027 ± 0.025±0.002	0.989	-0.002
0.230	9.93	−0.012 ± 0.016±0.001	0.989	-0.005	−0.024 ± 0.026±0.002	0.991	-0.002
0.259	10.77	−0.005 ± 0.017±0.001	0.992	-0.005	−0.010 ± 0.029±0.001	0.993	-0.002
0.292	11.70	0.026 ± 0.018±0.002	0.994	-0.004	0.009 ± 0.032±0.001	0.995	-0.002
0.328	12.64	−0.011 ± 0.020±0.002	0.995	-0.004	−0.008 ± 0.036±0.002	0.996	-0.002
0.369	13.61	0.036 ± 0.023±0.003	0.996	-0.004	0.043 ± 0.042±0.003	0.996	-0.002
0.415	14.55	0.016 ± 0.026±0.002	0.997	-0.003	0.060 ± 0.050±0.004	0.997	-0.002
0.467	15.56	−0.015 ± 0.031±0.003	0.998	-0.003	0.009 ± 0.062±0.003	0.998	-0.002
0.526	16.56	0.071 ± 0.038±0.004	0.998	-0.002	−0.125 ± 0.081±0.008	0.999	-0.001
0.591	17.55	0.045 ± 0.050±0.002	0.999	-0.002	0.023 ± 0.112±0.001	0.999	-0.002
0.666	18.49	−0.007 ± 0.070±0.000	0.999	-0.002	−0.188 ± 0.161±0.012	0.999	-0.002
0.749	19.45	0.094 ± 0.108±0.005	0.999	-0.002	0.338 ± 0.251±0.021	0.999	-0.002
0.844	20.45	0.309 ± 0.211±0.016	0.998	-0.002	0.240 ± 0.411±0.015	0.999	-0.003

TABLE II. Results for A_2 and xg_2 with statistical errors for proton and deuteron at the measured x and Q^2 [GeV^2]. The systematic error on xg_2 is given by $a + bx$ where $a_p(a_d)$= 0.0016(0.0009) and $b_p(b_d)$=−0.0012(−0.0008).

x	$< Q^2 >$	A_2^p	xg_2^p	A_2^d	xg_2^d
			$\theta \approx 2.75°$; E=29.1 GeV		
0.021	0.80	−0.015± 0.012	−0.037± 0.026	0.003± 0.017	0.009± 0.036
0.026	0.90	−0.009± 0.008	−0.026± 0.015	0.010± 0.011	0.020± 0.021
0.038	1.10	0.016± 0.006	0.020± 0.010	−0.013± 0.009	−0.021± 0.014
0.061	1.30	0.026± 0.008	0.017± 0.009	−0.017± 0.011	−0.024± 0.013
0.098	1.60	0.014± 0.010	−0.011± 0.009	0.025± 0.015	0.016± 0.013
0.155	1.80	0.061± 0.015	0.005± 0.010	0.008± 0.024	−0.005± 0.013
0.245	2.00	0.098± 0.024	−0.005± 0.010	0.058± 0.038	0.002± 0.014
0.380	2.10	0.258± 0.064	0.007± 0.018	−0.008± 0.105	−0.031± 0.024
			$\theta \approx 5.5°$; E=29.1 GeV		
0.061	2.70	0.033± 0.036	0.045± 0.061	0.059± 0.052	0.094± 0.084
0.098	3.50	0.029± 0.009	0.019± 0.013	0.000± 0.014	−0.009± 0.018
0.155	4.40	0.020± 0.008	−0.017± 0.009	0.024± 0.012	0.012± 0.012
0.245	5.30	0.042± 0.011	−0.021± 0.008	0.037± 0.017	0.000± 0.011
0.380	6.10	0.035± 0.019	−0.043± 0.007	0.086± 0.032	0.002± 0.010
0.580	6.70	0.107± 0.045	−0.020± 0.006	0.137± 0.082	−0.004± 0.008
0.780	7.00	−0.131± 0.130	−0.012± 0.003	0.444± 0.232	0.003± 0.004
			$\theta \approx 10.5°$; E=29.1 GeV		
0.155	7.10	0.030± 0.018	−0.001± 0.024	−0.023± 0.032	−0.042± 0.039
0.245	9.90	0.018± 0.016	−0.036± 0.016	0.029± 0.031	0.006± 0.025
0.380	13.10	0.054± 0.025	−0.026± 0.013	0.035± 0.052	−0.006± 0.021
0.580	16.30	0.090± 0.068	−0.010± 0.010	0.031± 0.156	−0.009± 0.017
0.780	18.40	−0.182± 0.259	−0.008± 0.005	0.795± 0.625	0.010± 0.009
			$\theta \approx 2.75°$; E=32.3 GeV		
0.021	0.80	−0.001± 0.008	−0.007± 0.020	0.003± 0.014	0.006± 0.031
0.026	0.90	0.002± 0.006	−0.004± 0.014	−0.006± 0.011	−0.010± 0.022
0.038	1.10	0.007± 0.005	0.001± 0.009	0.003± 0.008	0.006± 0.014
0.061	1.30	0.019± 0.006	0.009± 0.008	0.015± 0.010	0.015± 0.013
0.098	1.60	0.021± 0.009	−0.004± 0.008	−0.004± 0.014	−0.011± 0.013
0.155	1.80	0.045± 0.013	−0.008± 0.009	0.045± 0.021	0.015± 0.013
0.245	2.00	0.076± 0.020	−0.018± 0.009	0.063± 0.034	0.003± 0.014
0.380	2.10	0.209± 0.053	−0.004± 0.017	0.076± 0.095	−0.011± 0.025
			$\theta \approx 5.5°$; E=32.3 GeV		
0.061	2.70	−0.015± 0.023	−0.041± 0.042	0.046± 0.035	0.077± 0.061
0.098	3.50	0.017± 0.007	0.000± 0.011	0.004± 0.011	−0.003± 0.016
0.155	4.40	0.033± 0.007	−0.002± 0.008	0.028± 0.010	0.015± 0.011
0.245	5.30	0.041± 0.009	−0.023± 0.007	0.034± 0.015	0.003± 0.010
0.380	6.10	0.069± 0.016	−0.029± 0.007	0.000± 0.028	−0.024± 0.009
0.580	6.70	0.126± 0.038	−0.016± 0.005	0.078± 0.074	−0.008± 0.007
0.780	7.00	0.177± 0.110	−0.004± 0.003	0.170± 0.210	−0.002± 0.004
			$\theta \approx 10.5°$; E=32.3 GeV		
0.155	7.10	0.027± 0.013	0.001± 0.019	0.025± 0.022	0.019± 0.029
0.245	9.90	0.026± 0.012	−0.029± 0.013	0.006± 0.021	−0.016± 0.018
0.380	13.10	0.033± 0.019	−0.034± 0.010	−0.010± 0.035	−0.028± 0.015
0.580	16.30	0.000± 0.048	−0.024± 0.008	0.215± 0.105	0.013± 0.012
0.780	18.40	−0.146± 0.191	−0.008± 0.004	−0.527± 0.424	−0.011± 0.007
			AVERAGE		
0.021	0.80	−0.005± 0.007	−0.018± 0.016	0.003± 0.011	0.008± 0.023
0.026	0.90	−0.003± 0.005	−0.014± 0.010	0.002± 0.008	0.006± 0.015
0.038	1.10	0.011± 0.004	0.010± 0.007	−0.004± 0.006	−0.007± 0.010
0.061	1.40	0.020± 0.005	0.011± 0.006	0.003± 0.007	−0.001± 0.009
0.098	2.30	0.023± 0.004	−0.003± 0.005	0.006± 0.007	−0.001± 0.007
0.155	3.70	0.036± 0.004	−0.007± 0.004	0.026± 0.007	0.009± 0.006
0.245	5.00	0.048± 0.005	−0.022± 0.004	0.036± 0.009	0.000± 0.005
0.380	7.10	0.064± 0.009	−0.031± 0.004	0.029± 0.017	−0.015± 0.005
0.580	8.40	0.092± 0.023	−0.018± 0.003	0.122± 0.047	−0.004± 0.005
0.780	8.20	0.004± 0.074	−0.007± 0.002	0.228± 0.142	0.000± 0.002

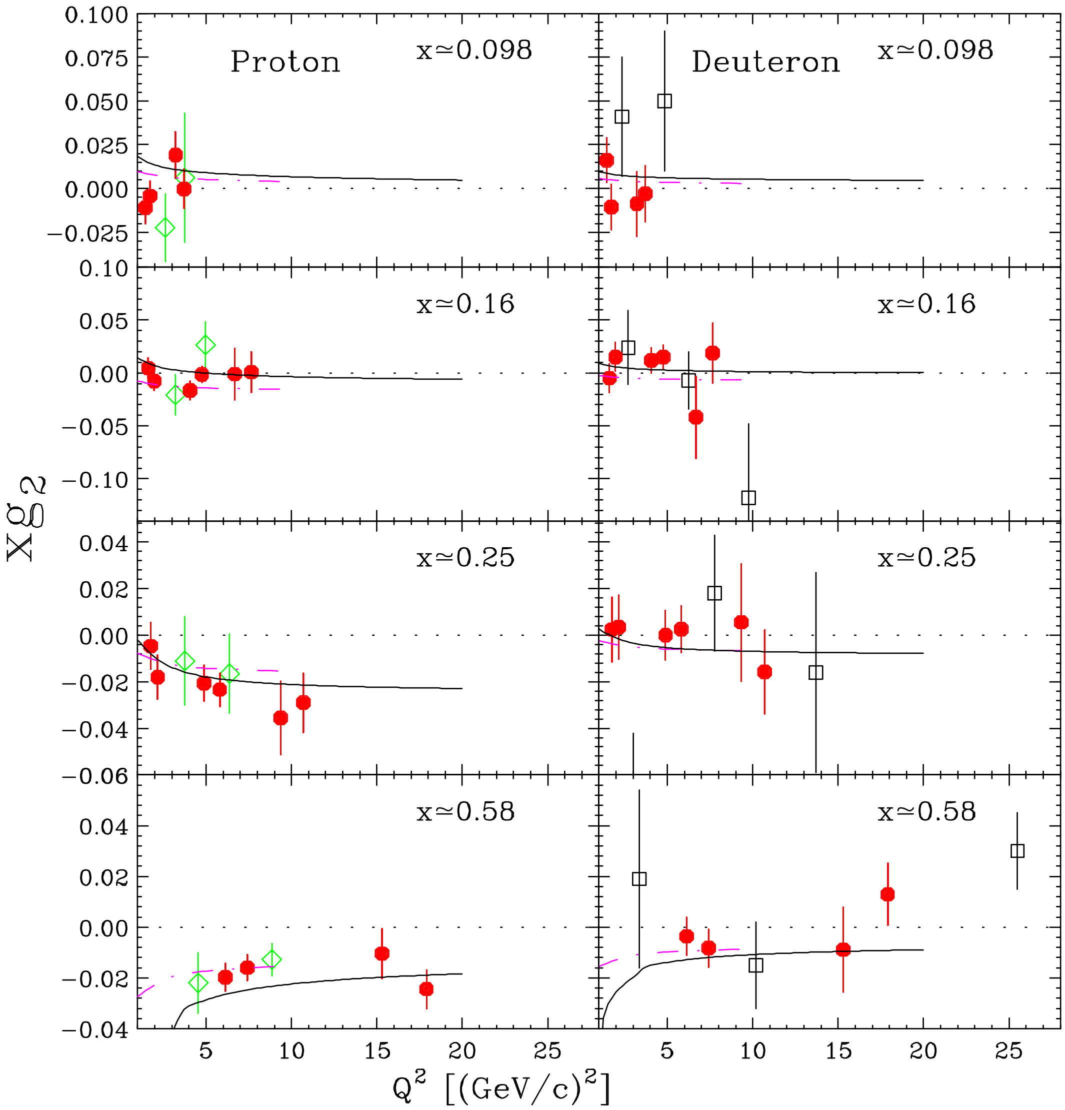

FIG. 1. xg_2 for the proton and deuteron as a function of Q^2 for selected values of x. Data are for this experiment (solid), E143 [6] (open diamond) and E155 [14] (open square). The errors are statistical; the systematic errors are negligible. The curves show xg_2^{WW} (solid) and the bag model calculation of Stratmann [19] (dash-dot).

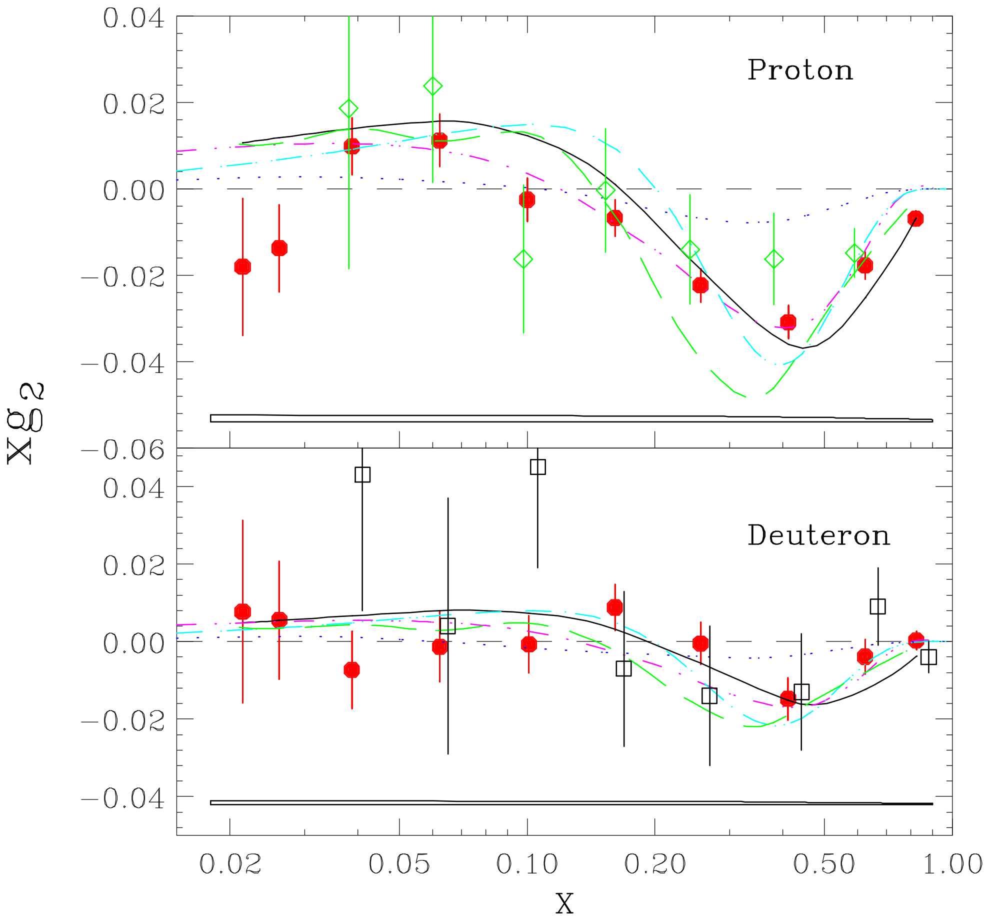

FIG. 2. The structure function xg_2 for all spectrometers combined (solid circle) and data from E143 [13] (open diamond) and E155 [14] (open square). The errors are statistical; the systematic errors are shown at the bottom. Also shown is our twist-2 g_2^{WW} at the average Q^2 of this experiment at each value of x (solid line). The curves are the bag model calculations of Stratmann [19] (dash-dot) and Song [11] (dot) and the chiral soliton models of Weigel and Gamberg [20] (short dash) and Wakamatsu [21] (long dash).

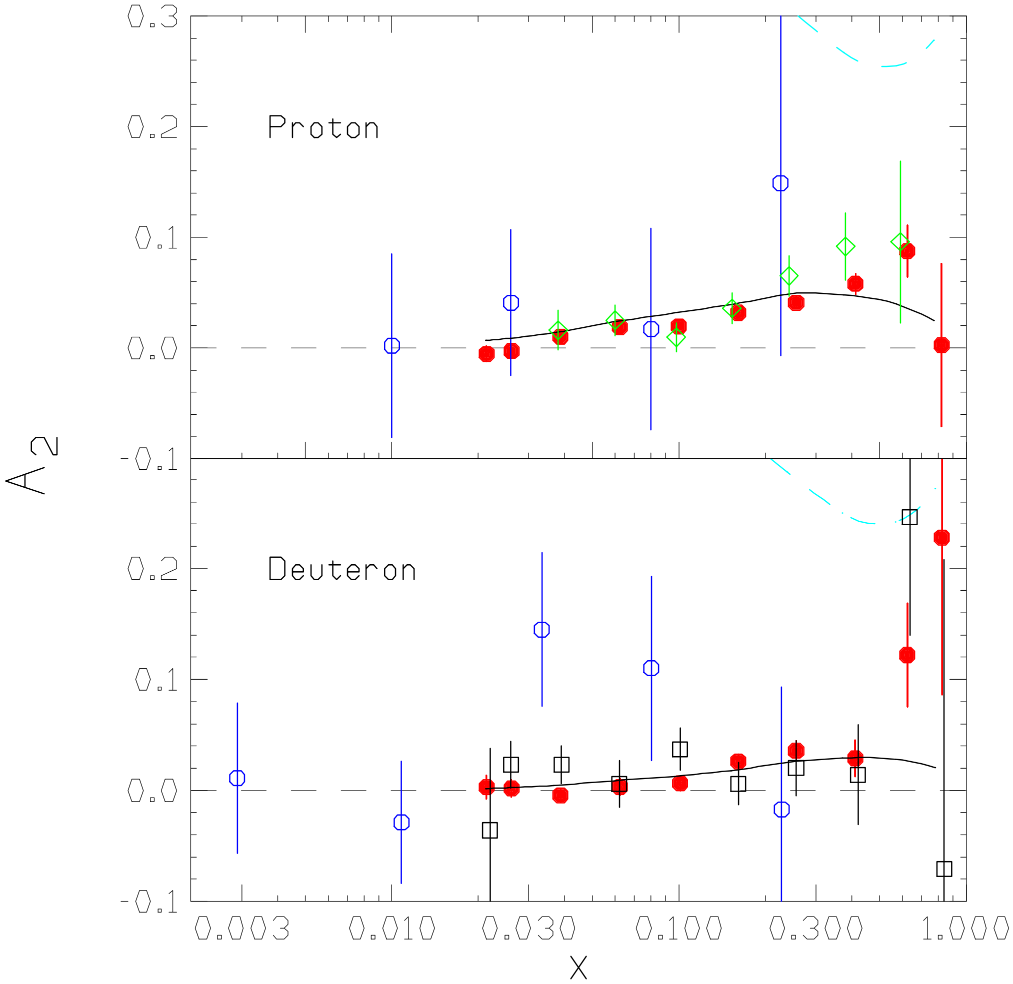

FIG. 3. The asymmetry A_2 for all spectrometers combined (solid circle) and data from E143 [13] (open diamond), E155 [14] (open square), and SMC [12] (open circles). The errors are statistical; the systematic errors are negligible. Also shown is A_2^{WW} calcultated from the twist-2 g_2^{WW} at the average Q^2 of this experiment at each value of x (solid line). The upper Soffer limit [22] is the dashed curve at the upper right.

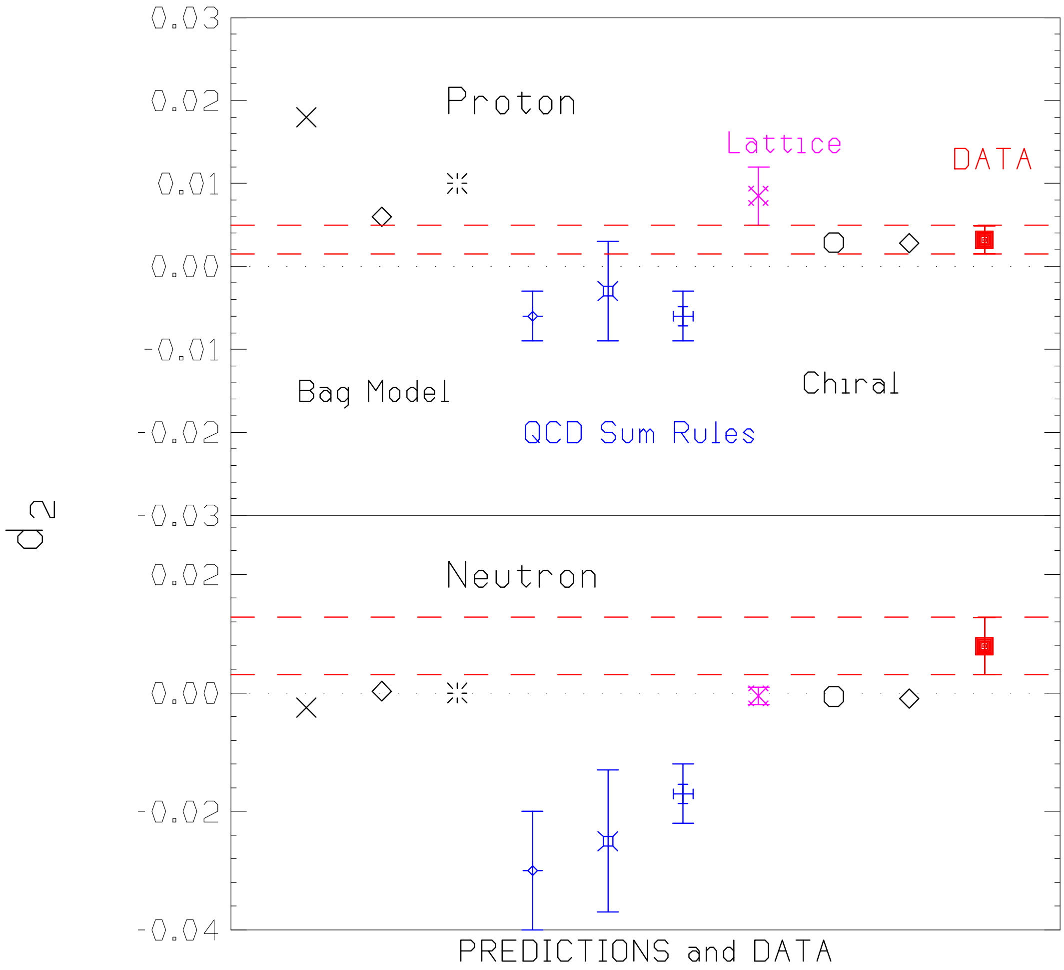

FIG. 4. The twist-3 matrix element d_2 for the proton and neutron from the combined data from SLAC experiments E142 [7], E143 [6], E154 [15] and E155 (Data). Also shown are theoretical model values from left to right: Bag Models [11,19,25], QCD Sum Rules [26–28], Lattice QCD [24] and Chiral Soliton Models [20,21]. The region between the dashed lines indicates the experimental errors.